AerospaceEurope Conference2021
WARSAW, POLAND | 23 -26 NOVEMBER 2021
CEAS Council of European Aerospace Societies

Model Predictive Control for Rigid Satellites Formation with Underactuated Propulsive System based on Relative Orbital Elements

Xingchuan Liu[1], Camilla Colombo[2], Francesca Scala[3], Danhe Chen [4]

[1)] School of Mechanical Engineering, Nanjing University of Science and Technology, 210094, Nanjing, China; acc_lxc@126.com
[2)] Department of Aerospace Science and Technology, Politecnico di Milano, 20156, Milano, Italy; camilla.colombo@polimi.it
[3)] Department of Aerospace Science and Technology, Politecnico di Milano, 20156, Milano, Italy; francesca1.scala@polimi.it
[4)]School of Mechanical Engineering, Nanjing University of Science and Technology, 210094, Nanjing, China; cranefeeling@hotmail.com

Abstract

This paper proposes a model predictive control approach for a rigid satellite formation maintenance scenario with tangential and normal forces based on relative orbital elements, under the propelling of the Formation Flying L-band Aperture Synthesis (FFLAS) mission concept, proposed by the European Space Agency. FFLAS intends to increase spatial resolution to improve meteorological and climate prediction with the incomparable advantages of formation. Considering the underactuated propulsive system equipped in satellites of FFLAS mission and time-variant relative inclination vector of this rigid formation, it is crucial to propose an automatic control approach to maintain this kind of satellite formation at nominal scientific phase with the requirements of high efficiency and optimal consumption. Model predictive control is selected as the fundamental automatic control way and the detailed implementation algorithm for time-variant system is described in this paper. Additionally, the discrete dynamic motion is created based on relative orbital elements and is decoupled to two subsystems, in plane and out of plane. Only the tangential force is used to manipulate the relative orbital elements in plane through reconstructed error of controlled objects after empirical analysis. Extensive simulations and comparative analysis are carried out to verify this proposed approach. The method demonstrates encouraging results, shows a remarkable performance compared with actuated propulsive system and the constraint solution for this underactuated system using the quadratic programming in terms of accuracy and consumption.

Keywords: underactuated system, rigid formation maintenance, model predictive control, relative orbital elements

1. Introduction

Satellite formation flying (SFF) is a majorly advance and constantly developing research field in space technology, causing some original applications in space mission. Multifarious attempts have been undertaken to achieve this kind of distributed mission architectures, with the advantages of reducing costs, development time, increasing safety and expanding possibilities for future mission concepts[1]. Various SFF missions have been launched to manifest rigorous stationkeeping, like the Magnetospheric Multi-Scale (MMS) mission from NASA, in which the spacecrafts achieved close separation of only four-and-a-half miles apart[2]. One that eminent is the CanX-4 & 5 mission for demonstrating autonomous configuration and maintenance by University of Toronto, first research mission to form an along-track orbit of 1000m, 500m, and a projected circular orbit of 100m, 50m, specifically for two nano satellites with propulsion subsystem of cold gas[3].

This study is conducted based on a SFF mission of FFLAS on a sun-synchronous orbit (SSO), development by the European Space Agency, Airbus, and Politecnico di Milano, intending to increase the imaging resolution for land and ocean applications by exploiting the virtual aperture given by the formation itself. This SFF mission includes three satellites, each of them would be equipped with propulsive system, which could provide the continuous forces in tangential and normal directions in the Local Vertical Local Horizontal (LVLH) coordinate frame. During the nominal scientific phase of SFF mission, it is pivotal to keep a rigid formation and a safe flight condition. Consequently, the automatic control approach is investigated for maintaining the nominal formation geometry with underactuated propulsive system, considering the orbital disturbance. This paper proposes a model predictive control approach for rigid satellite formation maintenance scenario with tangential and normal forces based on relative orbital elements. It’s mentionable that the separation distance of satellites is under 20 meters, which will be introduced in the following section.

This paper is dedicated to obtaining an automatic controller of efficiently and optimization. Automatic robust control methods have always been the pivotal technology for the proximity operation of SFF and spacecraft rendezvous, and numerous ways have been proposed by the scholars, such as linear quadratic regulator (LQR)[3], sliding mode control (SMC)[4], model predictive control (MPC)[5] and so on[6]. Up to now, plenteous control approaches have been derived for FF issues. However, most of researchers speculate that the satellites for proximity operation is fully actuated, which means that the dimension of the control input is equal to the number of the degrees of freedom to be controlled. In recent years, much attention has been paid to the underactuated satellites, considering the plenty of advantages to reduce the total mass of spacecraft and decrease the cost with fewer thrusters, especially for micro/nano satellites. And a number of control approaches have been developed such that the formation objective is achieved via various underactuated forms. Godard et al. [8] explored the feasibility of formation station keeping and reconfiguration with the loss of radial/in-track control by linear sliding mode (LSM) technique, and the resulting closed-loop control system presented global asymptotic convergence. Huang et al.[9] derived analytical solutions for the optimal underactuated satellite formation reconfiguration problem using indirect optimization methods with the minimum principle. Then, Huang et al. further designed another fast nonsingular terminal sliding mode controllers to deal with the under-actuated formation reconfiguration problem in the presence of unmatched disturbances[10]. Liu et al.[11] proposed an adaptive collision-free formation control strategy for a team of underactuated spacecraft subject to inertial parametric uncertainties. The adaptive control scheme was developed based on a hierarchical framework by potential function and Lyapunov theory. Nevertheless, all of them are based on the relative states and reckon without considering the optimization of consumption simultaneously.

MPC is an advanced control framework that optimizes predictive system behavior to determine the best current control input at each control step. It is also famous as receding horizon control, dynamical matrix control, and generalized predictive control. There are plenty of advantages to MPC implementation that influence its significant potential in the aerospace field. These advantages incorporate applicability to linear and nonlinear models, direct optimization of performance, handling of multivariable inputs and outputs, and systematic handling of multiple constraints. This kind of control have been applied for some space mission, for example, the Mars Sample Return (MSR) mission[12], which is the application of MPC towards spacecraft rendezvous of using a spacecraft to rendezvous and capture the soil from the Mars Ascent Vehicle (MAV) in a predefined orbit of Mars. Some scholars exploited the strategy and knowledge for proximity operation using MPC[13].

The paper is organized as follow. Section 2 provides the relative state and geometry feature of this FFLAS mission on the Hill orbital frame and describe the time-invariant trait in the relative orbital element framework. Section 3 introduces model predictive control implement solution for the time-variant system and the discrete dynamic model used to erect the control system based on relative orbital elements, decoupled two subsystems, in orbital plane and out of plane. Furthermore, an approach of formation maintenance under underactuated propulsive system in orbital plane is proposed. Section 4 presents the disturbance form and executes plenty of simulations to demonstrate the approach proposed under different combined coefficients, compared with actuated model and the constraint solution for this underactuated system using the quadratic programming. Finally, section 5 summarizes the work of this paper and presents future expectations.

2. Description of the rigid formation in FFLAS mission

The virtual center of FFLAS is selected an SSO at 775km of altitude, near circular orbit, with a local time of ascending node (LTAN) at 6:00 am. The task scenario of FFLAS is recommended by means of Hill orbital and relative orbital elements framework in detail, the rigid formation, and the control approach proposed is derived and applied for this task scenario. The formation is designed by COMPASS group in Politecnico di Milano, considering the balanced fuel consumption, sun shadowing effect, plume impingement, etc. And more details could be viewed in Ref 18.

2.1 Hill orbital framework

Hill orbital framework is utilized to describe the relative position of each satellite in formation, seen as Figure 1. The original center is located in the mass center of the chief satellite or a virtual center, which is regarded as the reference frame. Three vectors of T, N and R compose the coordinate axis. The vector T is aligned with the tangential direction of the reference orbit, the N is along the normal direction, and the R completes the right-handed Cartesian frame.

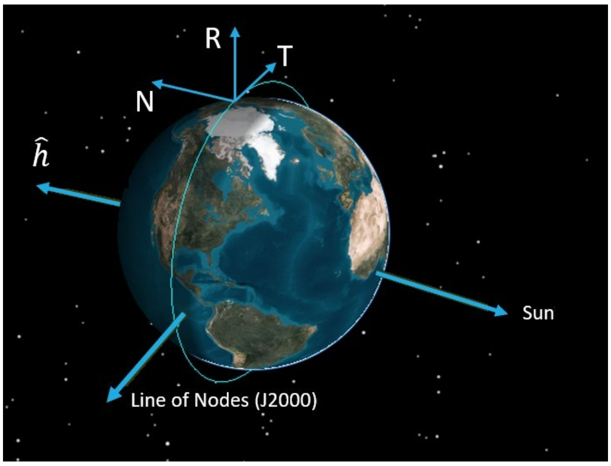

Figure 1 - The Hill orbital framework

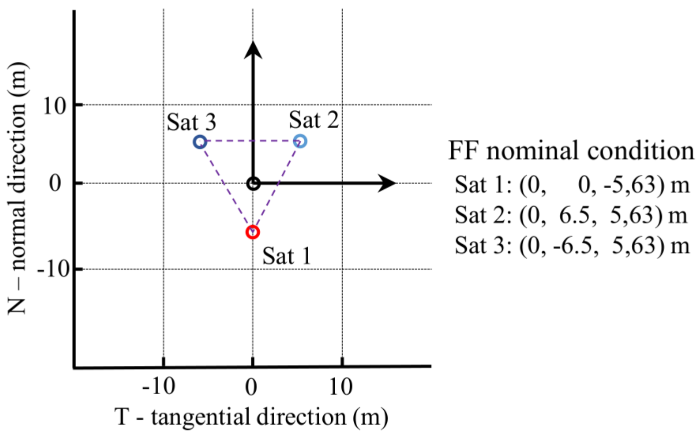

Figure 2 – The rigid formation nominal condition

The rigid formation mission of FFLAS in T-N plane during the nominal scientific period and the relative positions of three satellites are represented in Figure 2, including exact location data. Those satellites in the formation are identified as Sat 1, Sat 2, and Sat 3 respectively, placed at the vertex of an equilateral triangle of 13 m side. During the mission, the relative position of every deputy satellite is invariant, and the relative velocity is zero, which means the relative states of every satellite would be fixed referring to the virtual center and other satellites as the time of mission goes on.

2.2 Relative orbital elements framework

The ROEs describe the orbital elements of each satellite in the formation with respect to the reference orbit, a virtual center in this mission. Considering the mean classical Keplerian elements of the reference SSO and of a deputy satellite j of the formation as $\{a_c, e_c, i_c, \Omega_c, \omega_c, M_c\}$ and $\{a_d, e_d, i_d, \Omega_d, \omega_d, M_d\}$ respectively, the relative orbital elements are designed in Eq. (1).

$$\delta\boldsymbol{\alpha}=\begin{pmatrix}\delta a\\ \delta\lambda\\ \delta e_x\\ \delta e_y\\ \delta i_x\\ \delta i_y\end{pmatrix}=\begin{pmatrix}\delta a\\ \delta\lambda\\ \delta e\cos\varphi\\ \delta e\sin\varphi\\ \delta i\cos\theta\\ \delta i\sin\theta\end{pmatrix}=\begin{pmatrix}(a_d-a_c)/a_c\\ u_d-u_c+(\Omega_d-\Omega_c)\cos i_c\\ e_d\cos\omega_d-e_c\cos\omega_c\\ e_d\sin\omega_d-e_c\sin\omega_c\\ i_d-i_c\\ (\Omega_d-\Omega_c)\sin i_c\end{pmatrix} \tag{1}$$

where M is the mean anomaly, $u=\omega+M$ is the mean argument of latitude, $\delta\boldsymbol{e}=[\delta e_x, \delta e_y]$ and $\delta\boldsymbol{i}=[\delta i_x, \delta i_y]$ are the relative eccentricity and inclination vector, respectively.

The ROEs of Sat 3 are regarded as the hover scenario referring to the chief satellite in formation and analyzed to valid the approach proposed in term of tracking control. The ideal trajectory of ROEs is depicted in Figure 3. To make it clear to understand in geometry, the ROEs are represented in form of $a_c\delta\boldsymbol{\alpha}$. The ideal trajectory of relative inclination vector $a\delta\boldsymbol{i}$ is time-variant and other relative orbital elements are invariant, according to the analytical results. This study puts the emphasis on two aspects in this paper. The first one is the maintain control issue in orbital plane with underactuated propulsive system. The second one is the tracking control out of plane under time-variant ideal relative inclination vector $a_c\delta\boldsymbol{i}$.

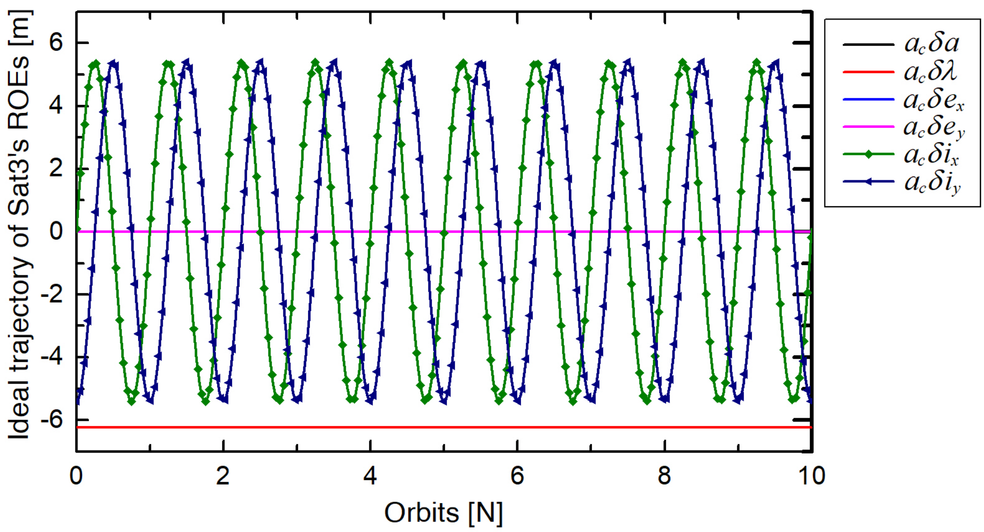

Figure 3 – Ideal trajectory of relative orbital elements of the Sat 3

3. Control strategy

In this subsection, the basic MPC implementation are introduced primarily. The basic structure of MPC is appropriate for the time-invariant control system, especially in the discrete dynamic model using relative orbital elements, due to the time-variant convolution matrix. Whereafter, linearized equation for ROEs and its discrete form are presented. Conveniently, the discrete dynamic is decoupled to two subsystems, in orbital plane and out of plane. Mentioned above, the subsystem in orbital plane needs to be controlled using only the tangential force. To solve this constraint problem, a novel method is derived that the discrete dynamic and error function for MPC implementation are reconstructed via further simplification, which would be more convenient to be executed for the micro calculator.

3.1 Model Predictive Control Implement for Time-variant System

MPC consists of an input horizon, a model of the plant behavior, and a minimized cost function to choose the current control input scheme. The choice of an input horizon depends on any significant dynamics in the system. The plant model is used to represent how the plant will respond given the future input horizon. The model must show the dependence of the plant response on the current measured variable and the future inputs from the input horizon to an accurate degree. The accuracy of the model depends on the application and errors that would arise from modeling the system behavior. The cost function is used as the criteria to determine which control action is best to choose. The cost function is the calculation that resolves the lowest numerical value to the cost.

For a time-varying discrete system, at each time t the model can also change over the prediction horizon. The general formulation of the model for SFF is expressed in Eq. (2) and (3):

$$\boldsymbol{X}(k+1)=\boldsymbol{A}(k)\boldsymbol{X}(k)+\boldsymbol{B}(k)\boldsymbol{U}(k) \tag{2}$$

$$\boldsymbol{Y}(k)=\boldsymbol{C}\boldsymbol{X}(k) \tag{3}$$

where, $X\in\mathbb{R}^{6\times6}$ denotes state vector of relative orbital elements, $\boldsymbol{U}\in\mathbb{R}^{3\times1}$ represents the input vector, $\boldsymbol{A}(k)\in\mathbb{R}^{6\times6}$ denotes the state transition matrix, and $\boldsymbol{B}(k)\in\mathbb{R}^{6\times3}$ represents the convolution matrix.

The purpose of control is to find out a set of predictive inputs $\hat{u}(k\,|\,k)$, $\hat{u}(k+1\,|\,k)$, … $\hat{u}(k+H_u-1\,|\,k)$, and predictive output $\hat{y}(k+1\,|\,k)$, $\hat{y}(k+2\,|\,k)$ … $\hat{y}(k+H_p\,|\,k)$, which make the objective function is minimum, based on the current output $y(k\,|\,k)$ and current input $u(k-1\,|\,k)$. The objective function is shown in Eq.(4),

$$V(k)=\sum_{i=1}^{H_p}\left\|\hat{y}(k+i\,|\,k)-r(k+i)\right\|^2_{Q(i)}+\sum_{i=0}^{H_{p-1}}\left\|\nabla\hat{u}(k+i\,|\,k)\right\|^2_{R(i)}, \tag{4}$$

where H_u is the control horizon, H_p is called the predictive horizon, $r(k)$ is the ideal reference trajectory, $Q(i)$ and $R(i)$ are the diagonal weighting matrix of states and control input respectively.

All predictive states could be obtained by the following equation,

$$\hat{\boldsymbol{X}}(k)=\boldsymbol{\Psi}(k)\boldsymbol{X}(k)+\boldsymbol{\Omega}(k)\boldsymbol{u}(k-1)+\boldsymbol{\Theta}(k)\Delta\hat{\boldsymbol{U}}(k), \tag{5}$$

where the vector $\hat{\boldsymbol{X}}(k)$ denotes all predictive states over predictive horizon H_p, the matrix $\boldsymbol{\Psi}(k)$ represents the transition matrix from initial state, the $\boldsymbol{\Omega}(k)$ denotes the influence matrix on predictive states by last step control input, and the $\boldsymbol{\Theta}(k)$ represents the influence matrix by every step control input increasement.

$$\hat{\boldsymbol{X}}(k)=\begin{bmatrix}\hat{x}(k+1|k)\\ \vdots\\ \hat{x}(k+H_u|k)\\ \hat{x}(k+H_u+1|k)\\ \vdots\\ \hat{x}(k+H_p|k)\end{bmatrix}_{H_p\times 1}, \tag{6}$$

$$\boldsymbol{\Psi}(k)=\begin{bmatrix}A_1\\ \vdots\\ A_{H_u}\\ A_{H_u+1}\\ \vdots\\ A_{H_p}\end{bmatrix}_{H_p\times 1}, \tag{7}$$

$$\Delta\boldsymbol{U}(k)=\begin{bmatrix}\Delta\hat{u}(k|k)\\ \vdots\\ \Delta\hat{u}(k+H_u-1|k)\end{bmatrix}_{H_u\times 1}, \tag{8}$$

$$\boldsymbol{\Omega}(k)=\begin{bmatrix}B_0\\ \vdots\\ \sum_{i=0}^{H_u-1}A_iB_{H_u-1-i}\\ \sum_{i=0}^{H_u}A_iB_{H_u-i}\\ \vdots\\ \sum_{i=0}^{H_p-1}A_iB_{H_p-1-i}\end{bmatrix}_{H_p\times 1}, \tag{9}$$

$$\boldsymbol{\Theta}(k)=\begin{bmatrix}B_0 & 0 & 0 & 0 & \cdots & 0\\ A_1B_0+B_1 & B_1 & 0 & 0 & \cdots & 0\\ A_2B_0+A_1B_1+B_2 & A_1B_1+B_2 & B_2 & 0 & \cdots & 0\\ \sum_{i=0}^{3}A_iB_{3-i} & \sum_{i=0}^{2}A_iB_{3-i} & \sum_{i=0}^{1}A_iB_{3-i} & B_3 & \cdots & 0\\ \vdots & \vdots & \vdots & \vdots & \vdots & \vdots\\ \sum_{i=0}^{j}A_iB_{j-i} & \cdots & \sum_{i=0}^{j-jj}A_iB_{j-i} & \cdots & \sum_{i=0}^{j-jj}A_iB_{j-i} & B_{Hu-1}\\ \cdots & \cdots & \cdots & \cdots & \cdots & A_iB_{Hu-1}+B_{Hu}\\ \cdots & \cdots & \sum_{i=0}^{j-jj}A_iB_{j-i} & \cdots & \cdots & \cdots\\ \vdots & \vdots & \vdots & \vdots & \vdots & \vdots\\ \sum_{i=0}^{H_p-1}A_iB_{H_p-1-i} & \cdots & \cdots & \cdots & \cdots & \sum_{i=0}^{H_p-H_u}A_iB_{H_p-H_u-i}\end{bmatrix}_{H_p\times H_u} \tag{10}$$

where A_i represents the transition matrix from initial state to i -th step predictive states in the huge matrix of $\boldsymbol{\Psi}(k)$ and $\boldsymbol{\Theta}(k)$, and B_j represents the convolution matrix at j -th step in the huge matrix of $\boldsymbol{\Theta}(k)$. Coherently, the symbol j represents the j-th row of the element, and jj represents the jj-th column of the element in huge matrix of $\boldsymbol{\Theta}(k)$. The detailed equations described above are utilized for the MPC implementation of time-invariant system.

The ideal trajectory is defined in Eq. (11), which has been obtained and shown in Figure 3.

$$\boldsymbol{\Gamma}(k)=\begin{bmatrix} r(k+1|k) \\ r(k+2|k) \\ \vdots \\ r(k+H_p|k) \end{bmatrix} \tag{11}$$

The objection function is described in Eq. (12) according to (4)

$$\boldsymbol{V}(k)=\left\|\hat{\boldsymbol{X}}(k)-\boldsymbol{\Gamma}(k)\right\|_{\boldsymbol{Q}}^{2}+\left\|\Delta\boldsymbol{U}(k)\right\|_{\boldsymbol{R}}^{2}. \tag{12}$$

The state errors are derived and depicted in Eq.(13),

$$\boldsymbol{\varepsilon}(k)=\boldsymbol{\Gamma}(k)-\boldsymbol{\Psi}(k)x(k)-\boldsymbol{\Omega}(k)\Delta\boldsymbol{U}(k-1). \tag{13}$$

The optimal control input increment sequence could be calculated by a classical solution without any constrained problems, shown in Eq. (14),

$$\Delta\boldsymbol{U}(k)_{opt}=\frac{1}{2}\boldsymbol{H}^{-1}\boldsymbol{G}, \tag{14}$$

where $\boldsymbol{G}=2\boldsymbol{\Theta}^{T}\boldsymbol{Q}\varepsilon(k)$, $\boldsymbol{H}=\boldsymbol{\Theta}^{T}\boldsymbol{Q}\boldsymbol{\Theta}+\boldsymbol{R}$.

In the rolling optimization strategy, the control input only adopts the first step of the solution, and at the next moment, a new optimal scheme will be figured out, which is the thought of rolling optimization. Therefore, the actual control input is the first vector of optimal input sequence, given by

$$\Delta\boldsymbol{u}_{inp}=\begin{bmatrix} I_{m\times m} & 0 & 0 & 0 \end{bmatrix}\Delta\boldsymbol{U}(k)_{opt}. \tag{15}$$

Generally, the MPC algorithm are usually used with quadratic programming solution to solve some constraint problems, such as the path constraint, control input constraint and so on, mainly in inequality form. In this paper, the lack of radial force could be regarded as one kind of control input constraint, whereas the thrust magnitude provided by the electronic engine could satisfy the requirement of maintenance of this rigid formation, unlike orbital transfer that remand great magnitude force. Therefore, as for the underactuated system in this scenario, the lack of force in radial direction becomes the only one constraint problem to be solved using quadratic programming. In order to improve efficiency, a reconstruct dynamic model is proposed to meet the MPC algorithm without using the quadratic programming to achieve precise control accuracy in condition of lack of force in radial direction.

To start using the control laws of MPC, the discrete dynamic model must first be defined. In next subsection, the actuated and underactuated discrete control model are described and introduced successively, based on the ROEs. The two discrete control models would be applied for the mission phase of FFLAS using the MPC strategy and the results would be analyzed and discussed in subsequent content. Underactuated discrete control model in orbital plane is derived according to the actuated model, but the error model is reconstructed and proposed for MPC implement in order to decrease the difficulty of calculation for automatic control.

3.2 Linearized Equation for ROEs and Discrete Actuated Control Model

According to the literature[7], this linearized equation is developed using the dimensionless relative orbit elements to determine the relative motion of one deputy satellite in terms of the chief satellite or the virtual center. For further simplifications, it's assumed that the chief is moving on a near-circular orbit, and the J2 perturbance is not considered in the relative motion due to the close distance. To linearize the equations of relative motion, it would need to be expanded to a first order differential equation using a Taylor series expansion and be centered about the chief orbit, depicted in Eq. (16).

$$\delta\dot{\boldsymbol{\alpha}}(t) = \boldsymbol{A}(\boldsymbol{\alpha}_c(t))\delta\boldsymbol{\alpha}(t) + \boldsymbol{B}(\boldsymbol{\alpha}_c(t))\delta\boldsymbol{\upsilon}(k) \tag{16}$$

The matrices $\boldsymbol{A}(\boldsymbol{\alpha}_c(t))$ and $\boldsymbol{B}(\boldsymbol{\alpha}_c(t))$ are shown below in Eq. (17) and (18).

$$\boldsymbol{A}(t) = \begin{bmatrix} 0 & 0 & 0 & 0 & 0 & 0 \\ -\frac{3}{2}n_c & 0 & 0 & 0 & 0 & 0 \\ 0 & 0 & 0 & 0 & 0 & 0 \\ 0 & 0 & 0 & 0 & 0 & 0 \\ 0 & 0 & 0 & 0 & 0 & 0 \\ 0 & 0 & 0 & 0 & 0 & 0 \end{bmatrix} \tag{17}$$

$$\boldsymbol{B}(t) = \frac{1}{na_c}\begin{bmatrix} 0 & 2 & 0 \\ -2 & 0 & 0 \\ \sin u_k & 2\cos u_k & 0 \\ -\cos u_k & 2\sin u_k & 0 \\ 0 & 0 & \cos u_k \\ 0 & 0 & \sin u_k \end{bmatrix} \tag{18}$$

$$\delta\boldsymbol{\upsilon}(k) = \begin{bmatrix} \delta\upsilon_R \\ \delta\upsilon_T \\ \delta\upsilon_N \end{bmatrix} \tag{19}$$

Where, the u_k is the mean argument of latitude of the chief orbit at the time of deputy satellite implementing impulse maneuver. $\delta\boldsymbol{\upsilon}(k)$ represents the control input impulse vector including three directions of radical, tangential, and normal.

For the implementation of MPC, the linear dynamics model should be discretized by being expressed as a function of the initial ROE vector, $\delta\boldsymbol{\alpha}(k)$, and the impulse vector $\delta\boldsymbol{\upsilon}(k)$, as shown in Eq. (20), which includes the state transition matrix $\boldsymbol{\Phi}(k)$, convolution matrix $\boldsymbol{\Gamma}(k)$, depicted in Eq. (21) and Eq. (22).

$$\delta\boldsymbol{\alpha}(k+1) = \boldsymbol{\Phi}(k)\delta\boldsymbol{\alpha}(k) + \boldsymbol{\Gamma}(k)\delta\boldsymbol{\upsilon}(k) \tag{20}$$

Without considering the J2 perturbance, the STM and convolution matrix related to the near-circular linear motion model is depicted in Eq. (21) and Eq. (22) .

$$\boldsymbol{\Phi}(k)=\begin{bmatrix} 1 & 0 & 0 & 0 & 0 & 0 \\ -\frac{3}{2}ndt & 1 & 0 & 0 & 0 & 0 \\ 0 & 0 & 1 & 0 & 0 & 0 \\ 0 & 0 & 0 & 1 & 0 & 0 \\ 0 & 0 & 0 & 0 & 1 & 0 \\ 0 & 0 & 0 & 0 & 0 & 1 \end{bmatrix} \tag{21}$$

$$\boldsymbol{\Gamma}(k)=\frac{1}{na_c}\begin{bmatrix} 0 & 2 & 0 \\ -2 & 0 & 0 \\ \frac{2}{\Delta u}\sin u_m \sin(\frac{\Delta u}{2}) & \frac{4}{\Delta u}\cos u_m \sin(\frac{\Delta u}{2}) & 0 \\ -\frac{2}{\Delta u}\cos u_m \sin(\frac{\Delta u}{2}) & \frac{4}{\Delta u}\sin u_m \sin(\frac{\Delta u}{2}) & 0 \\ 0 & 0 & \frac{2}{\Delta u}\cos u_m \sin(\frac{\Delta u}{2}) \\ 0 & 0 & \frac{2}{\Delta u}\sin u_m \sin(\frac{\Delta u}{2}) \end{bmatrix} \tag{22}$$

Where $dt = t - t_0$, that represents the duration time of the k th step for the discretized model. $u_m = \frac{u_k + u_{k+1}}{2}$ denotes the middle mean argument of latitude of the chief during deputy satellite implements maneuver from u_k to u_{k+1}, and $\Delta u = u_{k+1} - u_k$. $\delta \boldsymbol{\upsilon}(k)$ represents the control input impulse vector at period of dt including three directions of radical, tangential, and normal. It's assumed that the control input is constant thrust during the one step from t_0 to t for time and from u_k to u_{k+1} for mean argument of latitude of the chief. If the Δu is enough small, $\frac{2}{\Delta u}\sin(\frac{\Delta u}{2}) = 1$ in mathematics. It's worth to note that J2 perturbance is not considered in this discrete dynamic equation, due to the so close baseline of FFLAS mission.

3.3 Discrete Underactuated Control Subsystem for ROEs in orbital plane

The propulsion subsystem in the satellite of FFLAS mission only offers the force in tangential direction and normal direction. Consequently, it is very vital that how to achieve the automatic control problem with the underactuated subsystem.

The control model is decoupled system in orbital plane and normal direction according to the Eq.(20), which means that four relative orbital elements in plane of $\{\delta a,\ \delta\lambda,\ \delta e_x,\ \delta e_y\}$ are controlled by $\delta\upsilon_R$ and $\delta\upsilon_T$, two elements out of plane of δi_x and δi_y by $\delta\upsilon_N$ respectively. Due to lack of $\delta\upsilon_R$ and decoupled system, only the maintenance issue of four relative elements in plane is the one of most point of study, that is how to control this system via only the tangential impulse of $\delta\upsilon_T$. The underactuated control system in the orbital plane is reconstructed in Eq.(23).

$$\delta\tilde{\boldsymbol{\alpha}}(k+1) = \tilde{\boldsymbol{\Phi}}(k)\delta\tilde{\boldsymbol{\alpha}}(k) + \tilde{\boldsymbol{\Gamma}}(k)\delta\upsilon_T(k) \tag{23}$$

$$\delta\tilde{\boldsymbol{\alpha}} = \begin{bmatrix}\delta a & \delta\lambda & \delta e_x & \delta e_y\end{bmatrix}^T \tag{24}$$

$$\tilde{\boldsymbol{\Phi}}(t,t_0)=\begin{bmatrix} 1 & 0 & 0 & 0 \\ -\frac{3}{2}ndt & 1 & 0 & 0 \\ 0 & 0 & 1 & 0 \\ 0 & 0 & 0 & 1 \end{bmatrix} \tag{25}$$

$$\tilde{\boldsymbol{\Gamma}}(k)=\frac{1}{na}\begin{bmatrix}2\\0\\\frac{4}{\Delta u}\cos u_m\sin(\frac{\Delta u}{2})\\\frac{4}{\Delta u}\sin u_m\sin(\frac{\Delta u}{2})\end{bmatrix} \tag{26}$$

Form the Eq. (23), The $\delta\lambda$ could not be directly control by the tangential force, only affected by the relative semi-axis of δa and indirectly controlled by the tangential thrust. Furthermore, the discrete dynamic model for MPC implement is reconstructed, shown in Eq. (27). This model reduces the dimension of system and would make it more efficient to execute in on broad.

$$\delta\hat{\boldsymbol{\alpha}}(k+1)=\hat{\boldsymbol{\Phi}}(k)\delta\hat{\boldsymbol{\alpha}}(k)+\hat{\boldsymbol{\Gamma}}(k)\delta\upsilon_T(k) \tag{27}$$

$$\delta\hat{\boldsymbol{\alpha}}=\begin{bmatrix}\delta a & \delta e_x & \delta e_y\end{bmatrix} \tag{28}$$

$$\hat{\boldsymbol{\Phi}}(t,t_0)=\begin{bmatrix}1&0&0\\0&1&0\\0&0&1\end{bmatrix} \tag{29}$$

$$\hat{\boldsymbol{\Gamma}}(k)=\frac{1}{na}\begin{bmatrix}2\\\frac{4}{\Delta u}\cos u_m\sin(\frac{\Delta u}{2})\\\frac{4}{\Delta u}\sin u_m\sin(\frac{\Delta u}{2})\end{bmatrix} \tag{30}$$

Nonetheless, the element of $\delta\lambda$ in ROEs is neglected in system of Eq. (27). In order to guarantee the controllability for all of ROEs, the δa and $\delta\lambda$ are combined to one element to be controlled in this solution directly. This combined method is applied to obtain the control input using error equation in the above-mentioned MPC strategy, and the error equation applied is obtained via the reconstructed underactuated parameter, shown in Eq. (31) and Eq. (32).

$$\boldsymbol{\varepsilon}(k)=(\delta\hat{\boldsymbol{\alpha}}_0+\boldsymbol{\varepsilon}_{\Delta\delta\lambda})-\boldsymbol{\Omega}(k)\delta\hat{\boldsymbol{\alpha}}(k)-\boldsymbol{\Theta}(k)u \tag{31}$$

$$\boldsymbol{\varepsilon}_{\Delta\delta\lambda}=\begin{bmatrix}K_0(\delta\lambda_r-\delta\lambda_0) & 0 & 0\end{bmatrix}^T \tag{32}$$

Where K_0 is the combined coefficient, $K_0>0$, the $\delta\lambda_r$ and $\delta\lambda_0$ are the ideal and actual relative mean longitude respectively. In this way, the error of relative mean longitude would be controlled by means of bringing it to the error problem of relative semi-major axis. The stability of the MPC method based on this system could be proved via classical Lyapunov function referring to the method in Ref [15]. Therefore, the δa is leaded to convergence to the required rigid formation, and the $\delta\lambda$ would be leaded to convergence simultaneously. As for the parameter choice of K_0, if the parameter is excessive, it will make the system too sensitive for the error of $\delta\lambda$ that states oscillation and consumption waste happens. Therefore, it's critical to design a perfect parameter by numerical simulations.

3.4 Discrete Control Subsystem Out of Plane

Decoupled from the Eq. (20), the discrete model out of plane is yielded and shown in Eq. (33), which is very succinct in matrix dimensions and would make it more efficient that calculating the control law for the sake of the microcontroller by means of MPC.

$$\delta\breve{\boldsymbol{\alpha}}(k+1)=\breve{\boldsymbol{\Phi}}(k)\delta\breve{\boldsymbol{\alpha}}(k)+\breve{\boldsymbol{\Gamma}}(k)\delta\upsilon_N(k) \tag{33}$$

$$\breve{\boldsymbol{\Phi}}(t,t_0)=\begin{bmatrix}1&0\\0&1\end{bmatrix} \tag{34}$$

$$\breve{\boldsymbol{\Gamma}}(k)=\frac{1}{na_c}\begin{bmatrix}\frac{2}{\Delta u}\cos u_m\sin(\frac{\Delta u}{2})\\ \frac{2}{\Delta u}\sin u_m\sin(\frac{\Delta u}{2})\end{bmatrix} \tag{35}$$

As mentioned above, the ideal trajectory of inclination vector is time-variant, furthermore it will cause poor control error, especially in condition of large sampling time. From the view of relative states in Cartesian frame, the relative state in normal direction is constant, which always requires a constant thrust to maintain it. Therefore, the constant thrust would be derived in Cartesian frame18[14] and regarded as the initial control input for the implementation of MPC.

4. Simulation and Evaluation

In this section, the disturbance form only caused by non-spherical gravity are introduced and obtained by simulating with the input of orbital elements of FFLAS. Subsequently, the scenario and results are presented to testify the advancement and performance of the approach proposed.

4.1 Disturbance form

Affected by the J2~J6 perturbance of non-spherical gravity, the disturbance of relative orbital elements would be in some forms. Without losing generality, the formation with the capability of nature maintenance for a period of time is used to determine the disturbance form, which are the formation of space circular orbit with the radius of 50m. The disturbance would be higher order of magnitude than the formation mission of FFLAS, therefore the effective and capability of the method presented would be proved in the presence of external disturbance.

The orbit of chief satellite is identical with the mean orbit elements of virtual center of FFLAS mission, with the initial mean argument of latitude of zero, And the deputy satellite flies around the chief with the radius of 50m, using the method designed in Ref [16] to get the relative states and relative orbital elements. These output states of position and velocity obtained via numerical integration of RKF7(8) and propagation model [17] are used to determining each satellite's orbital elements in the inertial J2000 reference frame, after a chain of transformations comprising the nonlinear relationships between Cartesian states with Kepler orbital elements, and the conversations from osculating to mean elements, proposed in Ref [18]. During numerical integration, the atmosphere drag perturbation is neglected, for the reason of less difference in altitude of orbit and drag area.

The disturbance form in relative orbital elements is gained via the *cftool* of MATLAB, seen as Eq. (36). Conveniently, the emphasis of matching the curve is put on the magnitude, frequency and initial phase of *sin* forms. Then it would affect the next simulation scenario to demonstrate the automatic control approach proposed.

$$\begin{cases} D_{\delta a}=1.5\times10^{-4}\sin(3nT+3.91)\\ D_{\delta\lambda}=1.2\times10^{-4}\sin(3nT+2.46)\\ D_{\delta ex}=5\times10^{-4}\sin(4nT+4.185)\\ D_{\delta ey}=3\times10^{-4}\sin(4nT+0.98)\\ D_{\delta ix}=1\times10^{-5}\sin(3nT+0.69)\\ D_{\delta iy}=1\times10^{-5}\sin(3nT+5.28)\end{cases} m/s \tag{36}$$

Where, n is the mean angular velocity of the chief satellite. Incidentally, the disturbance extracted is utilized to demonstrate the proposed MPC method via a relatively simple approach. In Ref[1], Orekit was linked to offer the estimated states to prove the presented strategy including the perturbances, which would be perfect and complicated.

4.2 Simulation and Result Analysis in Orbital Plane

Based upon the previously described FFLAS mission, the rigid formation has been defined and are used to demonstrate the method by means of MPC strategy proposed. All the relative orbital elements and relative position are revealed in section 2, and the simulating duration is designed 10 orbital period of the chief satellite flying in the altitude of 775km. The error of control, consumption and control input are contrasted and analyzed with the actuated propulsive system, the constraint solution for this underactuated system using the quadratic programming (QP) and proposed underactuated model.

As for the basic parameters of MPC, the sampling time should be small enough to be able to produce a continuous force and approximate on-line in-orbit requirements but also long enough to reduce the predictive and control horizons to a number of steps computationally feasible within the on-board hardware. To demonstrate the proposed approach and study the relationship and the performance of the different combined coefficients, in term of consumption and accuracy in simulations, a total of six scenarios are utilized to analyze that, which incorporates actuated model, the way using the *quadprog* function to solve this constraint problems of lack of radial force, and the underactuated model with different parameters. Generally, the second method are frequently used to solve various of constraint problems, but more computational workload is required. All parameters have been presented in Table 1, which would be analyzed by following simulations.

Table 1 - Parameter value for formation maintenance in plane

Parameters		**Value**
Basic Parameters	Sampling time	16 s
	Predictive Horizon steps	32
	Control Horizon steps	16
Actuated	Thrust output weight	[1, 1]
	States divergence weight	[1, 1, 1, 1]
QP	Thrust output weight	[1, 1]
	States divergence weight	[1, 100, 1, 1]
Underactuated	Thrust output weight	1
	States divergence weight	[1, 1, 1]
	Combined coefficient K_0	50, 75, 100, 125

Firstly, the formation maintenance in plane is demonstrated due to the decouple dynamic motion. The result of the comparison of control accuracy between the actuated and underactuated model with the $K_0 = 50$ is shown in Figure 4. It shows the control error by means of MPC using the actuated and unactuated model. The magenta line represents the error under underactuated model, which means just only control thrust in the tangential direction. And the cyan line donates the error under actuated model using the control force in radial and tangential direction for maintenance the formation in plane. From the error result of the two way of control models, it is obvious to find that the error of the relative mean longitude using the unactuated model is much more exceptional than the actuated model, and the error range of the relative mean semi-major axis is comparable with another one. Inversely, the error range of the relative eccentricity vector using the unactuated model is twice as lager as another one.

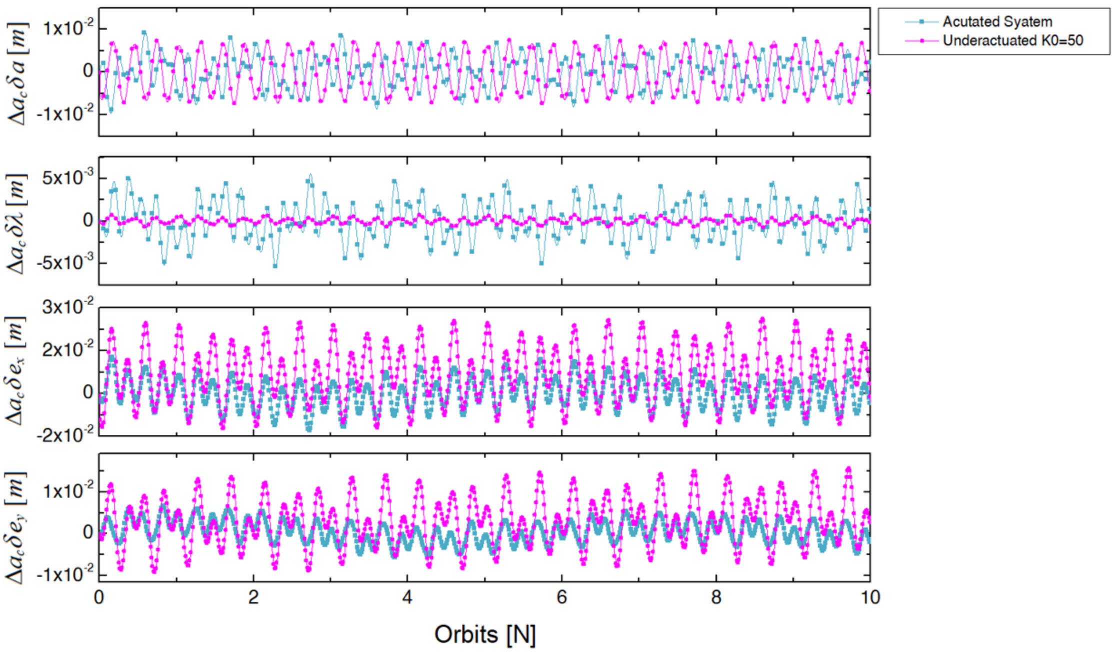

Figure 4 – The control accuracy comparison between underactuated and actuated approach.

Figure 5 represents the result of the comparison of control accuracy between the QP method and underactuated model. The magenta line represents the error under QP method, and the cyan line donates the error under underactuated model with the combined coefficient of $K_0 = 50$. From this figure, it is easy to find that the error of the relative mean longitude using the unactuated model is still more remarkable than the QP method, but the rest of errors are like the result of QP method. All error results of the evolution using underactuated model with the different combined coefficient is depicted in Figure 6. Unexpectedly, it's found that the error of ROEs in plane are identical, except the relative mean longitude. The error boundary of relative mean longitude is smaller in condition of the bigger combined coefficient.

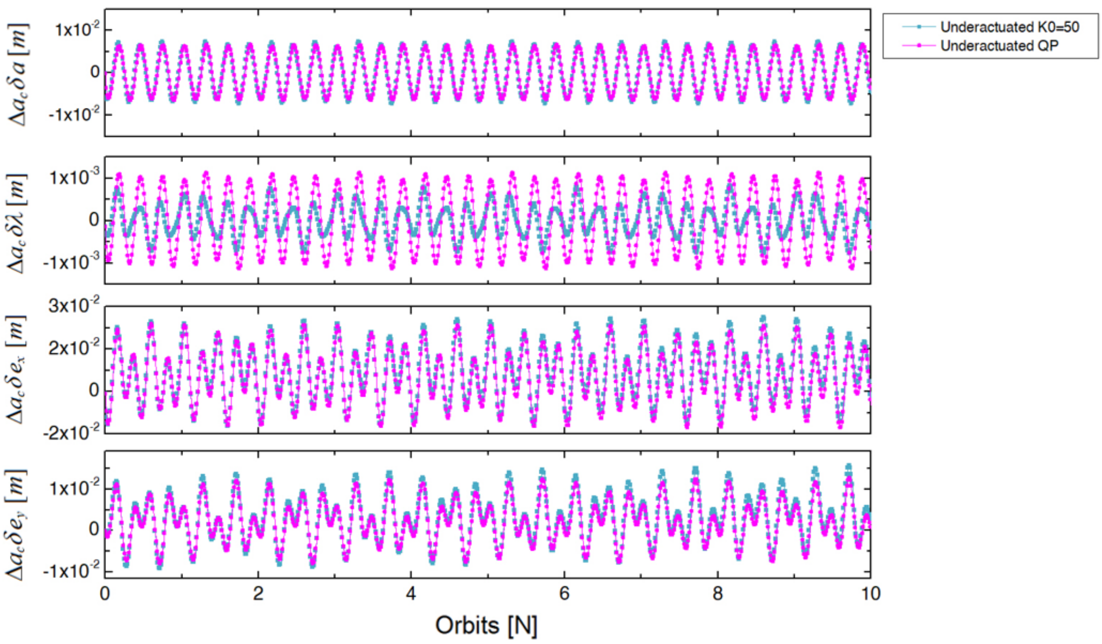

Figure 5 – The control accuracy comparison between underactuated and QR approach.

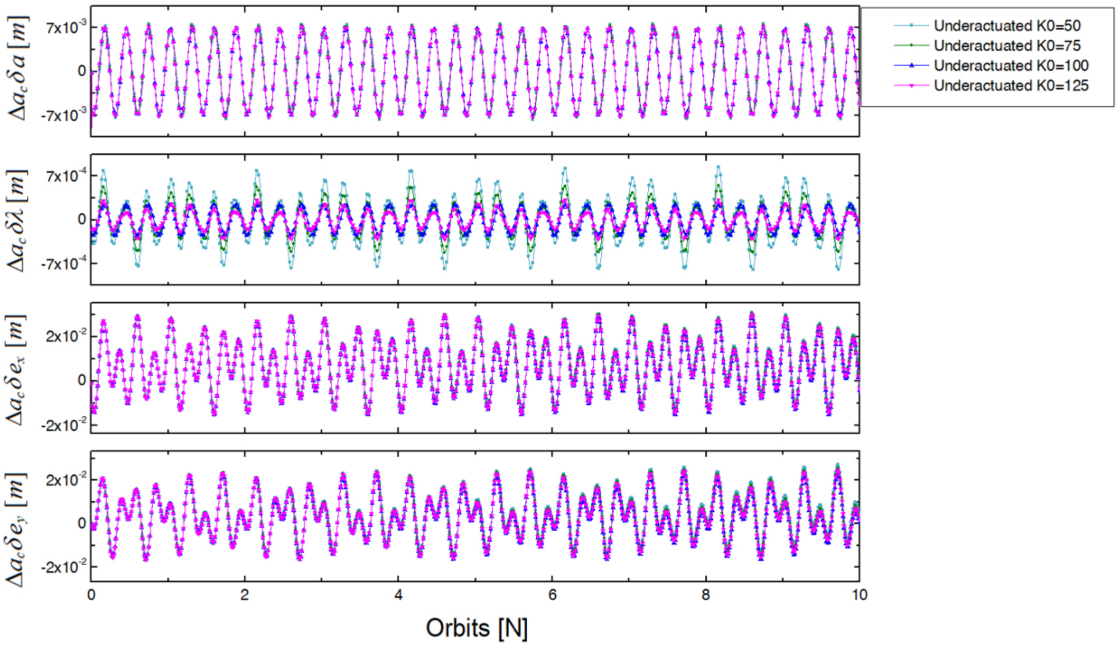

Figure 6 – The control accuracy comparison using the underactuated approach with four parameters.

During the formation maintenance for 10 orbital periods, the consumptions of thrust input for keeping the relative elements in plane referring to ideal trajectory with mentioned approaches are revealed in Figure 7. From this figure, all consumptions of four combined coefficients are little difference, and the consumption increases with the increasement of combined coefficient. Generally, the consumption of thrust input using the underactuated model is a little more than the actuated model, around 17~21% higher than the latter. The consumption of QP method is also a little more than the actuated model, just around 3.4% higher than the actuated model. Additionally, all the total consumptions for maintenance are very low, and less than 8×10^{-4} m/s, for the reason of the close formation and excellent performance of MPC. Nevertheless, comparing the difference in mass caused by the thrusters in radial direction, the mass of extra consumption of rigid formation maintenance by unactuated model is negligible.

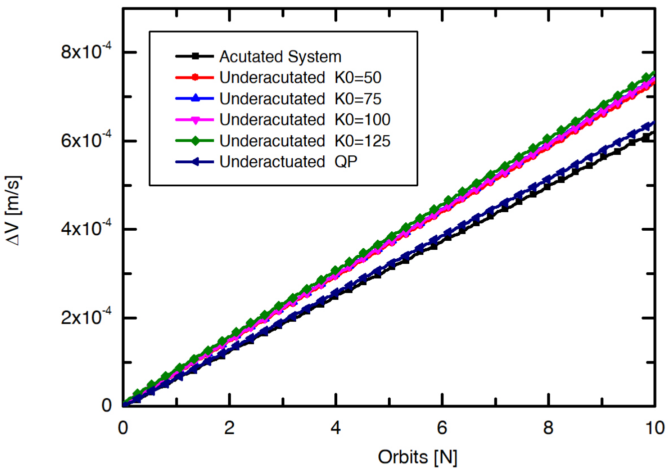

Figure 7 – The control consumption comparison in six cases.

Figure 8 shows the control inputs of all methods for the rigid formation maintenance, the input in radial and tangential direction using the actuated model, and the input in tangential direction using the underactuated model with different parameters and using QP method, it's worth to note that the input is in form of impulsive due to the sampling time of 16 sec and it is regarded as constant continuous force during one sampling time in the discrete model. Most of time, the magnitudes of all kinds of input are less than 4×10^{-4} m/s for 10 orbit periods. As a whole, the control input of all the method with underactuated system are equivalent to each other, whatever the magnitude and the overall form of input curve. Indeed, all the tangential inputs with underactuated system is more regular in contrast to the actuated one.

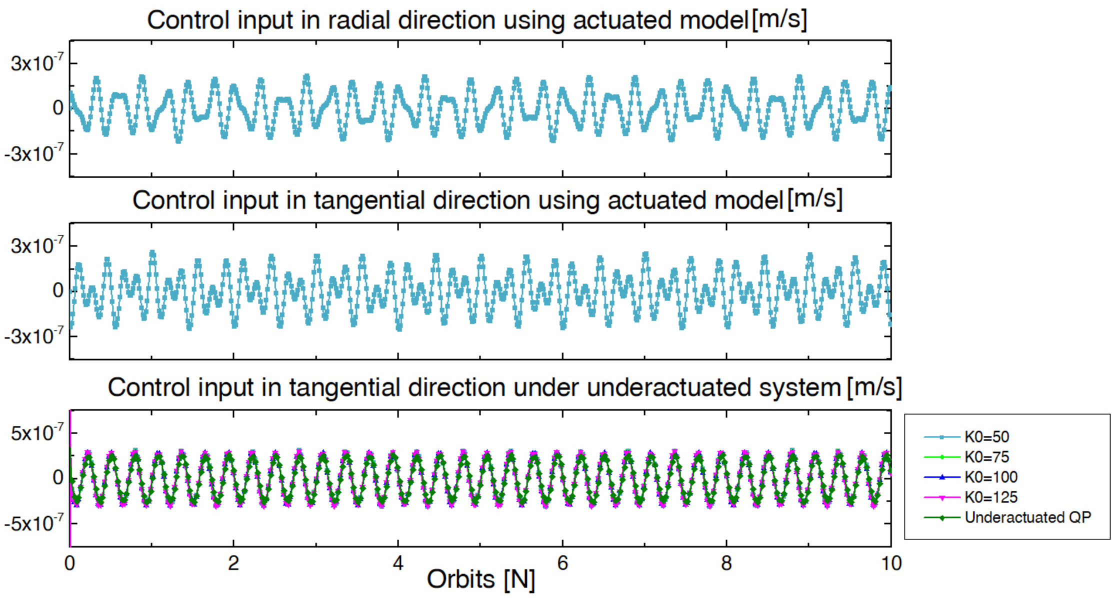

Figure 8 – The control inputs of six cases.

In contrast, the control inputs of underactuated models in incipient period are remarkable different with the QP method. To reveal the detail, all the inputs of first 20 sampling time are depicted in Figure 9, what should be noticed is that the larger combined coefficient causes the more obvious vibration, especially in the curve line of $K_0 = 125$. However, the control input obtained via QP method is enough smooth and stable, maybe this is the advantage of QP method. Finally, all the inputs via underactuated with the different parameters would become smooth and stable to match the external disturbance.

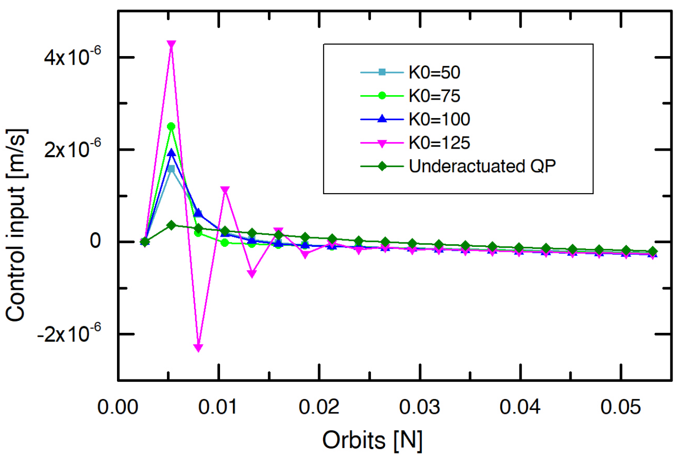

Figure 9 – The control inputs of the first 20 sampling time using the underactuated system.

In some literatures, the underactuated system is achieved through the inequation constraints and quadratic programming to solve the quadratic programming problem, which requires plenty of calculation to search the best control input to satisfy the demand of prioritization. This paper also presents this method to solve the underactuated problem and completes some comparisons and analysis between this method and proposed approach. According to those simulations and result, all conclusions could indicate that the proposed method has the wonderful performance for the formation maintenance. Unlike the orbital transfer, the magnitude of the thrust, which this rigid formation maintenance needs, is less than the magnitude provided by the thrusters. Only are the radial input zero as the constraint, that need to use the quadratic programming, which would have the disadvantage in term of computation speed, especially in so close formation.

4.3 Simulation and Result Analysis out of Plane

Based on the previously described FFLAS mission, the rigid formation causes the relative inclination vector is time-variant, which is very crucial for this mission, due to continuous control input in normal direction. The basic parameters of MPC and simulating duration are same as the previously mentioned, represented in Table 2.

Table 2 - Parameter value for formation maintenance out of plane

Parameters	**Value**
Sampling time	16 s
Predictive Horizon steps	32
Control Horizon steps	16
Thrust output weight	[1]
States divergence weight	[1, 1]

The control accuracy is shown in Figure 10. From that, the error of $a_c\delta i_x$ is within the boundary of $\pm 2\times 10^{-4}$ m and the error of $a_c\delta i_y$ is within the boundary of $\pm 1\times 10^{-4}$ m. Figure 11 depicts the control input data in this simulation. The input of control impulse changes in the range from 9.4075×10^{-5} to 9.41×10^{-5} m/s during one sampling of 16 sec, to match the time-invariant inclination vector in rigid formation and the external disturbance. And the total impulse of consumption is 0.3541 m/s, which means that it would cost 0.0354 m/s per orbital period. The wonderful performance of the MPC implement is demonstrated in the simulation.

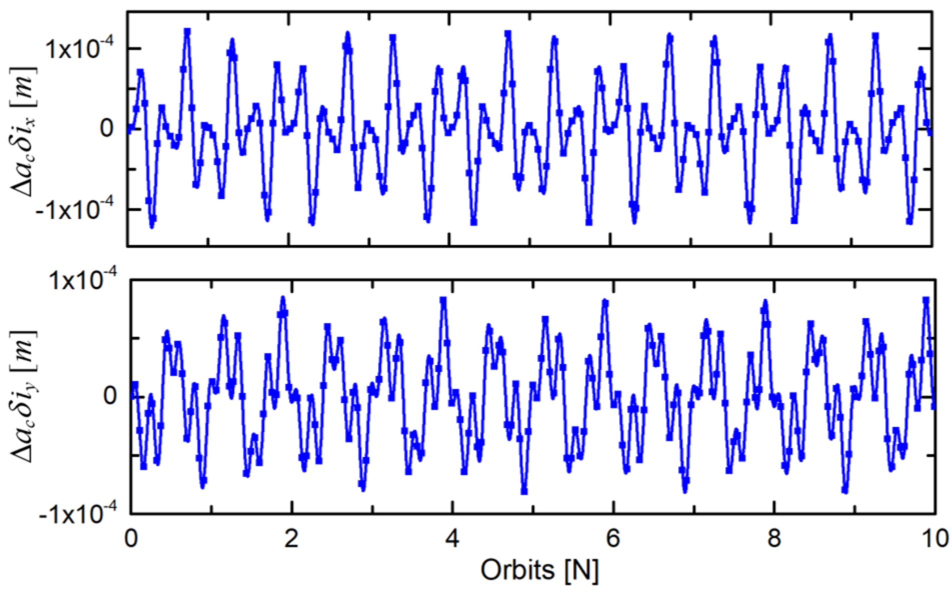

Figure 10 – The control accuracy of inclination vector using the MPC algorithm

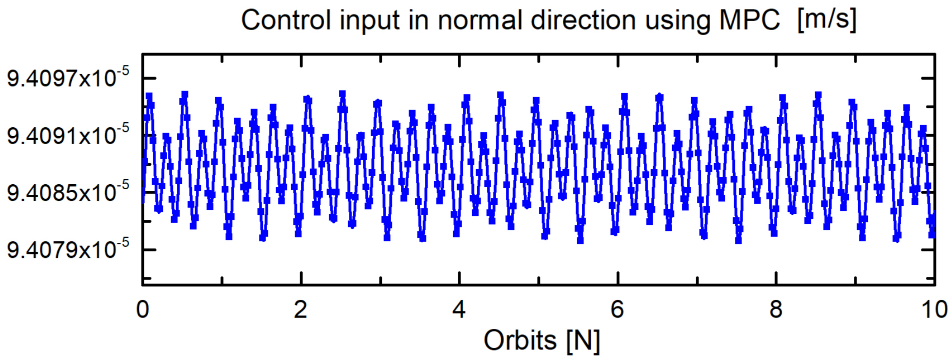

Figure 11 − The control input using the MPC algorithm

5. Conclusion

This paper proposes MPC as a suitable control strategy for FFLAS mission in LEO with underactuated propulsive system. In this paper, the direct algorithm of MPC is introduced for the time-invariant system based on ROEs, neglecting the J2 perturbation in dynamic model and constraints in MPC solution after analysis. Subsequent, the underactuated system in the orbital plane is reconstructed by combining the δa and $\delta\lambda$ to one element to be controlled in MPC by means of introducing a combined coefficient, while the error estimation method is proposed according to the reconstructed control system. To demonstrate the proposed approach, various of simulations are completed and the effects of the underactuated system and actuated system are compared in term of control accuracy, fuel consumption and control input, including the classical solution to solve constraint problems using MPC method and quadratic programming. As for out of plane, high precision control is revealed. The introduced approach demonstrates encouraging results, shows a remarkable performance compared with actuated propulsive system and the classical solution, and is operationally applicable in terms of computational expenses. In future, the performance of this method will be verified in the presence of practical engineering problems, such as the state determination noise.

Acknowledgements

The authors appreciates the financial support from the program of China Scholarships Council (No.202006840088), and this research has received funding of the research and innovation program (grant agreement No 679086 – COMPASS) from the European Research Council (ERC) under the European Union's Horizon 2020.

Copyright Statement

Reference

[1]. Scharnagl, J., Kremmydas, P., and Schilling, K. Model Predictive Control for Continuous Low Thrust Satellite Formation Flying. IFAC-PapersOnLine, Vol. 51(12), pp 12-17, 2018.

[2]. Sarah Frazier, NASA's MMS Achieves Closest-Ever Flying Formation, 2016, URL: https://www.nasa.gov/feature/goddard/2016/nasas-mms-achieves-closest-ever-flying-formation

[3]. Bonin, G., Roth, N., Armitage, S., Newman, J., Risi, B., and Zee, R.E. CanX-4 and CanX-5 Precision Formation Flight: Mission Accomplished. In Proceedings of the 29th Annual AIAA/USU Conference on Small Satellites. AIAA, Logan, UT, USA. 2015.

[4]. Cho, H., Udwadia F. E., and Wanichanon T. Autonomous Precision Control of Satellite Formation Flight under Unknown Time-Varying Model and Environmental Uncertainties. *The Journal of the Astronautical Sciences*, Vol 67(4), pp 1470-1499, 2020.

[5]. Hartley, E. N., Trodden, P. A., Richards, A. G., and Maciejowski J. M. Model predictive control system

design and implementation for spacecraft rendezvous. *Control Engineering Practice*, Vol. 20(7), pp 695-713, 2012.

[6]. Kristiansen, R., and Nicklasson, P. J. Spacecraft formation flying: A review and new results on state feedback control. *Acta Astronautica*, Vol 65(11-12), pp 1537-1552, 2009.

[7]. Erick Ausay, Model Predictive Control with Continuous Thrust for Spacecraft Formation Flying Applications, Master's Thesis, University of Florida, 2019.

[8]. Godard, K. Dev Kumar and A. Zou, Robust stationkeeping and reconfiguration of underactuated spacecraft formations. *Acta Astronautica*, Vol.105(2), pp 495-510, 2014.

[9]. Huang, X., Y. Yan and Y. Zhou, Analytical solutions to optimal underactuated spacecraft formation reconfiguration. Advances in Space Research, Vol. 56(10), pp 2151-2166, 2015.

[10]. Huang, X. and Y. Yan, Saturated Backstepping Control of Underactuated Spacecraft Hovering for Formation Flights. *IEEE transactions on aerospace and electronic systems*, Vol. 53(4), pp 1988-2000, 2017.

[11]. Liu, X., Z. Meng and Z. You, Adaptive collision-free formation control for under-actuated spacecraft. *Aerospace Science and Technology*, Vol. 79 pp 223-232, 2018.

[12]. Saponara, M., Barrena, V., Bemporad, A., Hartley, E., Maciejowski, J., Richards, A.,Tramutola, A., and Trodden, P., "Model Predictive Control Application to Spacecraft Rendezvous in Mars Sample Return Scenario," *Progress in Flight Dynamics, Guidance, Navigation, Control, Fault Detection, and Avionics*, EUCASS, St. Petersburg, Russia, Vol. 6, pp137–158, 2013.

[13]. Erick Ausay, Model Predictive Control with Continuous Thrust for Spacecraft Formation Flying Applications, Master's Thesis, University of Florida, 2019

[14]. F. Scala, G. Gaias, C. Colombo, Manuel Martìn-Neira. Formation Flying L-Band Aperture Synthesis: Design Challenges and Innovative Formation Architecture Concept, *71st International Astronautical Congress.*

[15]. Maciejowski, J. M. Predictive control: with constraints. Pearson education. pp. 167-172, 2002.

[16]. Sabol, C., R. Burns and C.A. McLaughlin, Satellite Formation Flying Design and Evolution. *Journal of Spacecraft and Rockets*, Vol. 38, No. 2, pp 270-278, 2001.

[17]. David A. Vallado. Fundamentals of Astrodynamics and Applications. Fourth Edition. Microcosm Press. pp. 593-595, 2013.

[18]. Gaias, G., C. Colombo and M. Lara, Analytical Framework for Precise Relative Motion in Low Earth Orbits. *Journal of Guidance, Control, and Dynamics*, Vol. 43, No. 5, pp 915-927, 2020.